Hypoxia inducible factor-prolyl hydroxylase inhibitor ameliorates the myopathy in a mice model of chronic kidney disease

Fang-Yuan Qian [1], Zuo-Lin Li [2], Yu-Dong Guo [3], Han-Chao Gao [4], Li-Hua Gu [1], Kai Le [1], Chun-Ming Xie [1*], Bin Wang [2*], Zhi-Jun Zhang [1*]

[1] Department of Neurology, Affiliated ZhongDa Hospital, School of Medicine, Southeast University, Nanjing, Jiangsu, China;

[2] Institute of Nephrology, ZhongDa Hospital, Southeast University School of Medicine, Nanjing, Jiangsu, China;

[3] Department of Orthopedic, Affiliated ZhongDa Hospital, School of Medicine, Southeast University, Nanjing, Jiangsu, China;

[4] Department of Nephrology, Shenzhen Longhua District Central Hospital, Guangdong Medical University Affiliated Longhua District Central Hospital, Shenzhen, China.

[*] These authors contributed equally to this work.

Correspondence to: Zhi-Jun Zhang, Department of Neurology, Affiliated ZhongDa Hospital, Medical School, Southeast University, No. 87 Dingjiaqiao Road, Nanjing, Jiangsu, China, 210009, E-mail: janemengzhang@vip.163.com.

Running head: HIF-PHI ameliorates the CKD myopathy in a mice model

Abstract

Muscle wasting and diminished physical performance contribute to the morbidity and mortality of chronic kidney disease (CKD), for which no curative therapy exists. Accumulating evidence indicates that impaired angiogenesis occurs in the muscles of CKD models. Pro-angiogenesis therapy is therefore considered a potentially effective

strategy for limiting CKD-associated myopathy. The hypoxia inducible factor-prolyl hydroxylase inhibitor (HIF-PHI) stabilizes HIF and enhances muscle angiogenesis during acute ischemia, however, little evidence was available from CKD models. Here, we assessed whether the pharmacological activation of HIF by MK-8617 (MK), a novel orally active HIF-PHI, improves CKD-associated myopathy. Mice were divided into Sham or CKD groups, and CKD mice were subdivided into CKD + vehicle or MK-treatment groups (1.5, 5 or 12.5 mg/kg for 12 weeks). In CKD mice, skeletal muscle mass, mitochondrial amount and exercise capacity decreased compared to Sham mice. Compared to the CKD + vehicle group, low (1.5 mg/kg) and medium (5 mg/kg) dose, but not high, significantly restored these changes and was accompanied by incremental increases in HIF-1α. Furthermore, increased capillary density and area were observed in a MK dose-dependent manner, which is likely related to an improved VEGF response in the skeletal muscle of CKD mice. In addition, macrophage and pro-inflammatory cytokines, including monocyte chemoattractant protein 1 (MCP-1), tumor necrosis factor (TNF-α) and interleukin 6 (IL-6), significantly increased in the high dose MK group. These results indicate that HIF-PHI provides a potential therapeutic strategy to improve CKD-associated myopathy.

Key-words: HIF-PHI, CKD-associated myopathy, angiogenesis, inflammation

Introduction

Muscle wasting and diminished physical performance are common

complications in chronic kidney disease (CKD), and strongly correlate with all-cause mortality of CKD (24, 30). Regarding to the complex mechanisms of myopathy induced by CKD, the abnormalities in the capillary bed of the skeletal muscle play an important role (4, 6, 25). To date, effective treatments for CKD-associated myopathy are lacking.

Hypoxia inducible factor (HIF) is a α/β heterodimeric transcription factor. It is constitutively expressed under well-oxygenated conditions, in which the prolyl hydroxylases (PHDs) can degrade it (17). However, under low oxygen conditions, the activity of PHDs is limited, and stabilized HIF transactivates multiple pro-angiogenic genes, including *vascular endothelial growth factor (VEGF)* (18), *VEGF receptor 1 (VEGFR1/FLT-1)* (15), and *erythropoietin (EPO)* (14).

Recent studies have reported that stabilized HIF induced angiogenesis in acute ischemia skeletal muscles in animal models (22, 26). In addition, previous evidence indicates that generation of new vasculature can strongly enhanced skeletal muscle regeneration in response to fiber injury in mice (21, 28). However, the effects of HIF stabilization on muscle in CKD-associated myopathy models have not been explored.

HIF-PHD inhibitors (HIF-PHIs) provide a pharmacological approach to stabilize HIF, and are undergoing clinical (and preclinical) trials for the treatment of CKD associated anemia (3, 27). We therefore tested the hypothesis that PHI would improve the impairment of muscle in CKD models. In this study, we used a range of doses of MK-8617 (MK) , which is a novel identified, orally active HIF-PHI, induces the stabilization of HIF-α through the inhibition of PHD 1-3 (5), to treat CKD mice for 12

weeks, focusing on changes in exercise capacity, muscle mass, mitochondria amount, angiogenesis and inflammatory status.

Materials and Methods

Animals

All animal procedures were approved by the Jiang Su Animal Care and Use Committee. C57BL/6J mice (5 weeks, male) were purchased from Vital River Laboratory Animal Technology Co., Ltd (Beijing, China) and were housed at a constant temperature with a 12-h light-dark cycle. All mice were provided free access to food and water.

CKD mice were produced through 5/6 nephrectomized (5/6 Nx) operations according to previous studies (32). The left kidney was initially decapsulated via left flank incision to avoid ureter and adrenal damage, and the upper and lower poles were resected. Bleeding was controlled through microfibrillar collagen (Avitene; Davol, Warwick, RI) and the upper and lower poles were weighed. After 1 week, the entire right kidney was decapsulated and removed via right flank incision. Sham-operated mice underwent surgery without damaging the kidneys.

Study Design

Twelve-week oral administration studies were performed with MK in mice. MK was obtained from Selleck Chemicals Inc. (Houston, USA). At 8 weeks after final surgery, CKD mice (n=6-8 per group) received vehicle [DMSO/PEG400/water (5:40:55, v/v/v)] or MK (1.5, 5 or 12.5 mg/kg in vehicle) by gavage once daily, and

Sham-operated mice (n=6) received gavage of vehicle once daily alone. Body weights were measured daily.

At 18 weeks, spontaneous motor activity and maximum hanging times were evaluated for all mice. After 2 weeks, muscle samples were collected from mice under anesthesia and weighted. Isolated muscle was mounted using tragacanth gum and snap frozen in liquid nitrogen-cooled 2-methylbutane. Samples were stored at −80°C. (See Figure 1 for the timelines.)

Serological parameters

Serum creatinine (C011-2, Jiancheng, Nanjing, China), blood urea nitrogen (BUN) (C013-2, Jiancheng, Nanjing, China) and hemoglobin (Hb) (A028-2, Jiancheng, Nanjing, China) levels were measured using commercial kits as per the manufacturer's protocols. Serum EPO (E-EL-M0027c 96T, R&D Systems, Minneapolis, MN) was measured using commercially available ELISA kits.

Behavioral tests

When performing the behavioral tests, experimental conditions were strictly controlled to minimize variation. Littermates were randomized across experimental groups. Animals were assessed by the same operator, who was blinded to the experimental groups. To control for odors and noises, tests were performed at the same time and day each weekday in the same room.

Open field tests

At the end of week 18, spontaneous motor activity was examined using open field apparatus for all mice. Briefly, each mouse was placed in the center of the open

field chamber (dimensions of 50 cm × 50 cm× 60 cm) and allowed to move freely for 5 min. A movement analysis system (Stoelting, IL, USA) was used to dissociate the activity time (s) and the total distance travelled (cm).The average speed (cm/s) was calculated by dividing the total distance travelled by the activity time. Between each trial, the chamber was wiped clean and dried.

Four limb hanging test

The maximum hanging time with four limbs was performed using previously described protocols (1). Animals were placed onto the lids of large cages and grids were positioned 25 cm above the soft bedding to prevent the mice from falling and to discourage them from intentionally jumping off the grid. The grid was secured so to remain stable and not impede the performance of the mice. Mice were placed on the grid and allowed to grasp it with all four paws. The grid was inverted so that the mice were hanging. The test session ended if mice were able to hang for 600 s. Mice that fell off the grid earlier were permitted a maximum of two further attempts.

Muscle immunohistochemistry

Factors influencing running and hanging times are multifactorial, including not only actual muscle strength but also animal motivation. Therefore, we detected the pathomorphism of the muscle to evaluate changes in the muscle itself. Only the mid-belly of each tibialis anterior muscle was used for histological studies, corresponding to one-third of the total muscle bulk. Hematoxylin and eosin (H&E) staining were performed as previously described (20). Succinate dehydrogenase (SDH) staining utilizing the activity of SDH, an enzyme of the mitochondrial respiratory

chain, were used to distinguish oxidative and non-oxidative fibers, which are indirect indicators of mitochondrial content, performed as previously described (13).

For immunohistochemistry, serial transverse 10-µm-thick cryosections were fixed with 4% formaldehyde and blocked in 5% fetal calf serum for 30 min. Sections were probed with primary anti-F4/80 (ab6640; Abcam) overnight at 4°C and labeled using a catalyzed signal amplification system and biotinylated secondary anti-mouse/rabbit antibodies (EliVision™ super kit) for macrophage detection. For immunofluorescence analysis, primary anti-CD31 antibodies (ab28364; Abcam) were used for capillary detection; anti-sarcoglycan (ab49811; Abcam) antibodies were used for muscle fiber detection; and anti-myosin heavy chain type IIA (SC-71; Developmental Studies Hybridoma Bank), IIX (6H1; Developmental Studies Hybridoma Bank), and IIB (BF-F3; Developmental Studies Hybridoma Bank) were used to detect fiber isoforms. All antibodies were incubated overnight at 4°C. Secondary antibodies for CD31 (ab150105; Abcam), Sarcoglycan (ab150075; Abcam) and Myosin heavy chain type (ab150075; Abcam) were incubated in the dark for 1 h at room temperature. Cell nuclei were stained with DAPI. Fluorescent images were obtained on an Olympus FV-1000 confocal microscope (Olympus, Japan) and non-fluorescent images were obtained on a Light Olympus BX51 microscope (Olympus, USA).

Transmission electron microscopy

To identify mitochondrial distributions in the muscle fibers, quadriceps were sliced into 1 mm^3 sections and fixed in 2.5% glutaraldehyde in 0.1 M cacodylate

buffer (pH 7.4, 4˚C, 48 hr). Tissue blocks were transferred to 1% osmium tetroxide in 0.1 M sodium cacodylate (PH 7.4) for 2 h, and stained in 2% aqueous uranyl acetate for a further 2 h. Following dehydration, tissue blocks were embedded in epoxy resin (Durcopan, Roth, Germany) and ultrathin sections of 40 nm thickness were cut using a Leica UC6 ultramicrotome (Leica, Wetzlar, Germany). Images were obtained on a H-7650 electron microscope.

Digital image analysis and morphometrics

Morphometry was performed by a single observer, blinded to the identity of the samples. An average of 10 frames were measured from each tissue section. A total of five hundred fibers per section were used to quantify the cross-sectional area (CSA) and SDH-positive fibers from three sections per animal were analyzed using Image-Pro Plus software (Media Cybernetics). SDH staining of muscle transverse sections were analyzed using ImageJ software (National Institute of Health). For the quantification of macrophages in muscle tissue slices, the average number of F4/80^{+} macrophages per millimeter square as counted from random images.

Capillaries were automatically counted after threshold mapping using Image-Pro Plus software. We measured the capillary area by analyzing the percentage of fluorescent pixels within each image for CD31, which was related to the percentage of fluorescent pixels for Sarcoglycan-γ within each image. Analysis of the capillary profiles included the capillary-to-fiber ratio and the mean capillary area.

RNA isolation and, qPCR

Total RNA from frozen gastrocnemius muscles was extracted by TRIzol (Takara) and precipitated in isopropanol. RNA quality and quantity were verified using a Nanodrop 2000 bioanalyzer (Thermo Scientific). Approximately, 4μg of RNA was reverse transcribed to cDNA using PrimeScript RT kits (Takara). Reactions were performed for 15 min at 37°C, 5 sec 85°C.

SYBR Green real-time quantitative PCRs (qRT-PCR) were performed using an ABI PRISM 7300 real-time PCR System (Applied Biosystems). VEGF, VEGF-R, monocyte chemoattractant protein 1 (MCP-1), tumor necrosis factor α (TNF-α) and interleukin 6 (IL-6) expression was calculated using the $2^{-\Delta\Delta Ct}$ method and normalized to β-actin. Primers were designed using Primer Express 3.0 (Applied Biosystems). Relative expression was normalized to β-actin levels. Specific primer sequences were as follows: VEGF-A(F) TCCTCTCCTTACCCCACCTCCT, VEGF-A(R) CTCACACACACAGCCAAGTCTCCT, VEGF-R1(F) ATTGAAAGAGTCACAGAGGAGGA, VEGF-R1(R) GAGTTAGAAGGAGCCAAAAGAGG, VEGF-R2(F) GCACTCTCCACCTTCAAAGTCTCAT, VEGF-R2(R) GTATTCCCCTTGGTCACTCTTGGTC, MCP-1(F) CATCCACGTGTTGGCTCA, MCP-1(R) GATCATCTTGCTGGTGAATGAGT, TNF-α(F) TCTTCTCATTCCTGCTTGTGG, TNF-α(R) GGTCTGGGCCATAGAACTGA, IL-6(F) GATGGATGCTACCAAACTGGAT and IL-6(R) CCAGGTAGCTATGGTACTCCAGA.

The PCR conditions were as follows: 95°C for 30 s; 95°C for 5 s, 60°C for 31 s, for 40 cycles; 95°C for 15 s, 60°C for 1 min, 95°C for 15 s, and 60°C for 15 s.

Western blot analysis

Tissues from the gastrocnemius muscle were homogenized using RIPA lysis buffer supplemented with 10mM NaF, 1mM Na_3VO_4, 1 mM phenylmethylsulfonyl fluoride and protease inhibitors (Roche, Indianapolis, IN, USA) for 30 min on ice. Lysates were centrifuged at 15000 rpm for 30 min at 4°C and protein concentrations were determined through BCA assays (Thermo Scientific, USA). Equal protein concentrations were resolved on 12% SDS-PAGE gels and transferred to nitrocellulose membranes. Membranes were blocked in 5% milk TBST (20 mM Tris-HCl, 150 mM NaCl, pH7.6) containing 0.1% (vol/vol) Tween 20 at room temperature for 1 h. Membranes were probed with primary antibodies in blocking solution overnight at 4°C and labeled with anti-HIF-1α (ab2185; Abcam), anti-VEGF-A (ab1316; Abcam) and anti-GAPDH (CW0100M, CWBio, China) antibodies. Membranes were labeled with the appropriate HRP-conjugated secondary antibodies and visualized using enhanced chemiluminescence detection reagents (Millipore, Billerica, MA, USA). The levels of phosphorylated proteins were calculated relative to total protein expression or actin using ImageJ software.

Statistical analyses

Groups were compared using unpaired t-tests. The means for each group were compared through an analysis of variance followed by Tukey's multiple comparisons. $P < 0.05$ was considered statistically significant.

Results

MK ameliorates spontaneous motor activity, maximum hanging times and muscle atrophy in CKD mice at low or medium dose

Serum creatinine (SCr) and blood urea nitrogen (BUN) significantly increased in CKD + vehicle mice compared to Sham + vehicle mice (Table 1), indicating successful production of the CKD model.

As previously reported (9, 11), HIF-1α levels were significantly lower in the gastrocnemius muscle of CKD + vehicle mice compared to Sham + vehicle mice (Figure 2A). As predicted, the expression of HIF-1α increased in a dose-dependent manner in mice treated with MK (Figure 2A).

The running speed and maximal hanging time of CKD + vehicle mice significantly declined compared to Sham + vehicle mice (Figure 2B-C). Furthermore, a significant reduction in both body and muscle weight of CKD + vehicle mice was observed (Table 1). H&E staining of the myofiber cells indicated a reduction in size in the tibialis anterior (TA) muscles of CKD + vehicle mice (Figure 2D). Quantification of the myofiber size revealed an increase in the proportion of smaller myofibers and a reduction in the proportion of larger myofibers in CKD + vehicle mice (Figure 2E). The mean fiber area significantly decreased in CKD + vehicle mice either (Figure 2F). These deteriorations were suppressed by the administration of low (1.5 mg/kg), medium (5 mg/kg), but not high (12.5 mg/kg) doses of MK (Figure 2B-F).

The number of mitochondria-rich oxidative fibers significantly decreased in CKD + vehicle mice (Figure 3A-B, Supplemental Figure S1

https://figshare.com/s/979700db0c1ff74f9199). Electron microscopy showed that the mitochondrial numbers decreased and mitochondrial hypertrophy was evident in the muscles of CKD + vehicle mice (Figure 3D-F). The number of oxidative fibers and mitochondria significantly increased in response to low, medium, but not high MK dose (Figure 3A-B, Supplemental Figure S1 https://figshare.com/s/979700db0c1ff74f9199). Furthermore, a reduction in mitochondrial size was observed at all MK doses (Figure 3A-F).

MK promotes angiogenesis in the skeletal muscle of CKD mice

Capillary density and area significantly increased in CKD mice administrated MK (Figure 4A-C). Higher levels of VEGF-A and lower levels of VEGF-R1/2 were observed in the muscles of CKD + vehicle mice (Figure 4D-G). Intriguingly, high doses of MK, but not low or medium dose increased VEGF-A expression at the mRNA and protein level (Figure 4D, G). Low, medium and high MK doses also enhanced the expression of VEGF-R1 in CKD mice (Figure 4E). The serum levels of EPO also significantly increased in MK treated CKD mice (Table 1).

High dose of MK promote inflammation in the muscles of CKD mice

As shown in Figure 5A-B, high dose of MK increased the number of macrophages infiltration to the muscles. Furthermore, the levels of MCP-1 (Figure 5C), IL-6 (Figure 5D) and TNF-α (Figure 5E) remarkably increased in the muscles of CKD mice administered high dose of MK.

Discussion

This study confirmed that skeletal muscle mass and exercise capacity are

severely reduced in the presence of impaired kidney function. Furthermore, we showed that muscle impairment can be ameliorated by stimulating the HIF system, which may be related to promoted angiogenesis in skeletal muscle of CKD mice. Taken together, our findings demonstrated that HIF-PHI might be a promising therapeutic agent for improving CKD-associated myopathy.

Muscle wasting and diminished physical activity are common during the early stages of CKD (12, 30). Tamaki et al. found that young CKD mice (16–20 weeks, 9–13 weeks after 5/6 Nx operation) had decreased muscle mitochondria and exercise capacity but preserved muscle volume (29). Older mice (48–52 weeks, 41–45 weeks after 5/6 Nx operation) lost muscle volume and exercise capacity, in addition to a loss of skeletal muscle mitochondria (8, 29). In contrast, significantly lower HIF-1α expression and capillary density were observed in the skeletal muscle of mice during early (4 weeks after 5/6 Nx operation) and persistent CKD stages (12 weeks after 5/6 Nx operation) (2, 9-11). In this study, we examined an intermediate stage of CKD mice (20 weeks after 5/6 Nx operation) and compared their characteristics to Sham mice. We found that the exercise capacity of the mice significantly declined and muscle weights significantly decreased. In addition, muscle HIF-1α levels significantly decreased. The number of mitochondria significantly decreased and was accompanied by mitochondrial hypertrophy, whilst both the capillary density and area decreased. The administration of MK to the CKD mice significantly increased muscle HIF-1α levels and restored exercise capacity, muscle mass, the levels of mitochondria and mitochondrial hypertrophy at specific doses. These findings suggest that the

administration of HIF-PHI may aid the recovery of impaired CKD muscle.

The potential mechanism(s) underlying these changes are complex and multifactorial. Our findings showed that daily MK administration for 12 consecutive weeks promoted muscular angiogenesis in CKD mice potentially through the activation of HIF-regulated pro-angiogenic factors, including VEGF-A, VEGFR1 and EPO (18, 26). It is well known that any increase in muscle capillarity is important in enhancing oxygen delivery and removal of metabolites to/from tissues, which can enhance the function of muscle (21, 28). Thus, the amelioration of impaired CKD muscle may be related to the improved muscular angiogenesis. On the other hand, Yang et al. showed that augmentation of HIF activity accelerated muscle stem cell self-renewal in hypoxic environments (31). In addition, improvement of renal function accompanied by a reduced production of uremic toxins improved CKD-induced muscle atrophy and contributed to improved exercise capacity (8). Moreover, the whole body angiogenesis could also been improved and contribute to improved performances in the open field test and limb hanging test. Further investigation will be necessary to delineate the full spectrum of contributing mechanisms.

Interestingly, we found that IL-6 was increased in the high dose MK group. The effects of IL-6 on muscle wasting in CKD are controversial (7, 16, 23). In several studies, it has been reported that IL-6 induced muscle wasting (7), whilst others demonstrated that IL-6 facilitated local immune cell infiltration which in turn upregulated IGF-1 to limit muscle wasting in CKD models (16). Moreover, Raj et al.

found that increased IL-6 was associated with increased muscle protein synthesis during hemodialysis in patients with end-stage renal disease (23). Therefore, the effect of increased IL-6 expression in high doses of MK on skeletal muscle needs to be further investigated in the present models.

Recently, Debenham et al. evaluated the off target activity of MK to establish specificity (5). *In vitro*, they demonstrated that MK was a significant inhibitor of PHD 1-3, and the IC50 was 1.0, 1.0 and 14 nM, respectively. MK was inactive when IC50 > 60 μM against the cytochrome p450 enzymes, as well as other 171 radioligand binding and enzymes when screened at 10 μM. In addition, no off-target effects were reported when mice received a daily single oral dose of 5 or 15 mg/kg for MK (5). These data suggested that MK has very good selectivity for PHDs both *in vitro* and *in vivo*. Based on the above data, we speculated that in normal mice, PHDs were specific targets of MK, although the off-target effect of MK in Sham mice needs to be further confirmed.

In summary, we demonstrated that HIF-PHI is a powerful angiogenic pharmaceutical agent that can prevent muscle atrophy in CKD mice. Despite this potential, harmful side effects can occur and optimal therapeutic doses must be identified. Further studies are now required to dissect the molecular mechanism(s) regulating the effects of HIF-PIH and the translation of these findings to human studies.

Acknowledgments

We thank Mr. Guang-ming Gan and Mrs. Chen-chen Zhang from School of Medicine, Southeast University, for the support of the confocal microscope and transmission electron microscope guidance.

Disclosures

All authors claim that there are no conflicts of interest.

Grants

This study was supported by the Jiangsu Provincial Medical Outstanding Talent (JCRCA2016006) and the Fundamental Research Funds for the Central Universities and the Scientific Research Innovation Program for College and University Graduates of Jiangsu Province (KYLX16_0300).

References:

1. **Aartsma-Rus A, and van Putten M**. Assessing functional performance in the mdx mouse model. *J Vis Exp* 2014.
2. **Acevedo LM, Peralta-Ramirez A, Lopez I, Chamizo VE, Pineda C, Rodriguez-Ortiz ME, Rodriguez M, Aguilera-Tejero E, and Rivero JL**. Slow- and fast-twitch hindlimb skeletal muscle phenotypes 12 wk after (5/6) nephrectomy in Wistar rats of both sexes. *Am J Physiol Renal Physiol* 309: F638-F647, 2015.
3. **Chen N, Hao C, Peng X, Lin H, Yin A, Hao L, Tao Y, Liang X, Liu Z, Xing C, Chen J, Luo L, Zuo L, Liao Y, Liu BC, Leong R, Wang C, Liu C, Neff T, Szczech L, and Yu KP**. Roxadustat for Anemia in Patients with Kidney Disease Not Receiving Dialysis. *N Engl J Med* 2019.
4. **D'Apolito M, Du X, Pisanelli D, Pettoello-Mantovani M, Campanozzi A,**

Giacco F, Maffione AB, Colia AL, Brownlee M, and Giardino I. Urea-induced ROS cause endothelial dysfunction in chronic renal failure. *ATHEROSCLEROSIS* 239: 393-400, 2015.

5. **Debenham JS, Madsen-Duggan C, Clements MJ, Walsh TF, Kuethe JT, Reibarkh M, Salowe SP, Sonatore LM, Hajdu R, Milligan JA, Visco DM, Zhou D, Lingham RB, Stickens D, DeMartino JA, Tong X, Wolff M, Pang J, Miller RR, Sherer EC, and Hale JJ**. Discovery of N-[Bis(4-methoxyphenyl)methyl]-4-hydroxy-2-(pyridazin-3-yl)pyrimidine-5-carboxa mi de (MK-8617), an Orally Active Pan-Inhibitor of Hypoxia-Inducible Factor Prolyl Hydroxylase 1-3 (HIF PHD1-3) for the Treatment of Anemia. *J MED CHEM* 59: 11039-11049, 2016.

6. **Di Marco GS, Reuter S, Hillebrand U, Amler S, Konig M, Larger E, Oberleithner H, Brand E, Pavenstadt H, and Brand M**. The soluble VEGF receptor sFlt1 contributes to endothelial dysfunction in CKD. *J AM SOC NEPHROL* 20: 2235-2245, 2009.

7. **Du J, Mitch WE, Wang X, and Price SR**. Glucocorticoids induce proteasome C3 subunit expression in L6 muscle cells by opposing the suppression of its transcription by NF-kappa B. *J BIOL CHEM* 275: 19661-19666, 2000.

8. **Enoki Y, Watanabe H, Arake R, Fujimura R, Ishiodori K, Imafuku T, Nishida K, Sugimoto R, Nagao S, Miyamura S, Ishima Y, Tanaka M, Matsushita K, Komaba H, Fukagawa M, Otagiri M, and Maruyama T**. Potential therapeutic interventions for chronic kidney disease-associated sarcopenia via indoxyl

sulfate-induced mitochondrial dysfunction. *J Cachexia Sarcopenia Muscle* 8: 735-747, 2017.

9. **Flisinski M, Brymora A, Bartlomiejczyk I, Wisniewska E, Golda R, Stefanska A, Paczek L, and Manitius J**. Decreased hypoxia-inducible factor-1alpha in gastrocnemius muscle in rats with chronic kidney disease. *Kidney Blood Press Res* 35: 608-618, 2012.

10. **Flisinski M, Brymora A, Elminowska-Wenda G, Bogucka J, Walasik K, Stefanska A, Odrowaz-Sypniewska G, and Manitius J**. Influence of different stages of experimental chronic kidney disease on rats locomotor and postural skeletal muscles microcirculation. *Ren Fail* 30: 443-451, 2008.

11. **Flisinski M, Wisniewska-Chudy E, Brymora A, Stefanska A, Strozecki P, and Manitius J**. Chronic kidney disease leads to hypoxia inducible factor-1alpha to hypoxia inducible factor-2alpha switch in the gastrocnemius muscle. *J PHYSIOL PHARMACOL* 68: 419-425, 2017.

12. **Fried LF, Lee JS, Shlipak M, Chertow GM, Green C, Ding J, Harris T, and Newman AB**. Chronic kidney disease and functional limitation in older people: health, aging and body composition study. *J AM GERIATR SOC* 54: 750-756, 2006.

13. **Fujita N, Nagatomo F, Murakami S, Kondo H, Ishihara A, and Fujino H**. Effects of hyperbaric oxygen on metabolic capacity of the skeletal muscle in type 2 diabetic rats with obesity. *ScientificWorldJournal* 2012: 637978, 2012.

14. **Haase VH**. Regulation of erythropoiesis by hypoxia-inducible factors. *BLOOD REV* 27: 41-53, 2013.

15. **Harris AL**. Hypoxia-a key regulatory factor in tumour growth. *NAT REV CANCER* 2: 38-47, 2002.

16. **Hu L, Klein JD, Hassounah F, Cai H, Zhang C, Xu P, and Wang XH**. Low-frequency electrical stimulation attenuates muscle atrophy in CKD-a potential treatment strategy. *J AM SOC NEPHROL* 26: 626-635, 2015.

17. **Kaelin WJ, and Ratcliffe PJ**. Oxygen sensing by metazoans: the central role of the HIF hydroxylase pathway. *MOL CELL* 30: 393-402, 2008.

18. **Kao R, Xenocostas A, Rui T, Yu P, Huang W, Rose J, and Martin CM**. Erythropoietin improves skeletal muscle microcirculation and tissue bioenergetics in a mouse sepsis model. *CRIT CARE* 11: R58, 2007.

19. **Kelly BD, Hackett SF, Hirota K, Oshima Y, Cai Z, Berg-Dixon S, Rowan A, Yan Z, Campochiaro PA, and Semenza GL**. Cell type-specific regulation of angiogenic growth factor gene expression and induction of angiogenesis in nonischemic tissue by a constitutively active form of hypoxia-inducible factor 1. *CIRC RES* 93: 1074-1081, 2003.

20. **Kim HJ, Kim NC, Wang YD, Scarborough EA, Moore J, Diaz Z, MacLea KS, Freibaum B, Li S, Molliex A, Kanagaraj AP, Carter R, Boylan KB, Wojtas AM, Rademakers R, Pinkus JL, Greenberg SA, Trojanowski JQ, Traynor BJ, Smith BN, Topp S, Gkazi AS, Miller J, Shaw CE, Kottlors M, Kirschner J, Pestronk A, Li YR, Ford AF, Gitler AD, Benatar M, King OD, Kimonis VE, Ross ED, Weihl CC, Shorter J, and Taylor JP**. Mutations in prion-like domains in hnRNPA2B1 and hnRNPA1 cause multisystem proteinopathy and ALS. *NATURE*

495: 467-473, 2013.

21. **Mofarrahi M, McClung JM, Kontos CD, Davis EC, Tappuni B, Moroz N, Pickett AE, Huck L, Harel S, Danialou G, and Hussain SN**. Angiopoietin-1 enhances skeletal muscle regeneration in mice. *Am J Physiol Regul Integr Comp Physiol* 308: R576-R589, 2015.

22. **Niemi H, Honkonen K, Korpisalo P, Huusko J, Kansanen E, Merentie M, Rissanen TT, Andre H, Pereira T, Poellinger L, Alitalo K, and Yla-Herttuala S**. HIF-1alpha and HIF-2alpha induce angiogenesis and improve muscle energy recovery. *EUR J CLIN INVEST* 44: 989-999, 2014.

23. **Raj DS, Moseley P, Dominic EA, Onime A, Tzamaloukas AH, Boyd A, Shah VO, Glew R, Wolfe R, and Ferrando A**. Interleukin-6 modulates hepatic and muscle protein synthesis during hemodialysis. *KIDNEY INT* 73: 1054-1061, 2008.

24. **Roshanravan B, Robinson-Cohen C, Patel KV, Ayers E, Littman AJ, de Boer IH, Ikizler TA, Himmelfarb J, Katzel LI, Kestenbaum B, and Seliger S**. Association between physical performance and all-cause mortality in CKD. *J AM SOC NEPHROL* 24: 822-830, 2013.

25. **Sakkas GK, Ball D, Sargeant AJ, Mercer TH, Koufaki P, and Naish PF**. Skeletal muscle morphology and capillarization of renal failure patients receiving different dialysis therapies. *Clin Sci (Lond)* 107: 617-623, 2004.

26. **Schellinger IN, Cordasic N, Panesar J, Buchholz B, Jacobi J, Hartner A, Klanke B, Jakubiczka-Smorag J, Burzlaff N, Heinze E, Warnecke C, Raaz U, Willam C, Tsao PS, Eckardt KU, Amann K, and Hilgers KF**. Hypoxia inducible

factor stabilization improves defective ischemia-induced angiogenesis in a rodent model of chronic kidney disease. *KIDNEY INT* 91: 616-627, 2017.

27. **Semenza GL**. Pharmacologic Targeting of Hypoxia-Inducible Factors. *Annu Rev Pharmacol Toxicol* 59: 379-403, 2019.

28. **Shimizu-Motohashi Y, and Asakura A**. Angiogenesis as a novel therapeutic strategy for Duchenne muscular dystrophy through decreased ischemia and increased satellite cells. *FRONT PHYSIOL* 5: 50, 2014.

29. **Tamaki M, Miyashita K, Wakino S, Mitsuishi M, Hayashi K, and Itoh H**. Chronic kidney disease reduces muscle mitochondria and exercise endurance and its exacerbation by dietary protein through inactivation of pyruvate dehydrogenase. *KIDNEY INT* 85: 1330-1339, 2014.

30. **Wang XH, and Mitch WE**. Mechanisms of muscle wasting in chronic kidney disease. *NAT REV NEPHROL* 10: 504-516, 2014.

31. **Yang X, Yang S, Wang C, and Kuang S**. The hypoxia-inducible factors HIF1alpha and HIF2alpha are dispensable for embryonic muscle development but essential for postnatal muscle regeneration. *J BIOL CHEM* 292: 5981-5991, 2017.

32. **Yu R, Chen JA, Xu J, Cao J, Wang Y, Thomas SS, and Hu Z**. Suppression of muscle wasting by the plant-derived compound ursolic acid in a model of chronic kidney disease. *J Cachexia Sarcopenia Muscle* 8: 327-341, 2017.

Figure Legends

Figure 1. Schematic evaluating the effects of different MK doses on CKD mice. C57/6J mice (♂, 5 weeks) were produced through a two-step surgical process.

Eight-weeks after surgery, mice were assigned to Sham + vehicle [DMSO/PEG400/water (5:40:55, v/v/v)], CKD + vehicle, CKD + 1.5 mg/kg, 5 mg/kg or 12.5 mg/kg MK groups, respectively. After 18 weeks of surgery, behavioral tests were performed. Two weeks after the behavioral tests, mice were sacrificed, and blood and skeletal muscle tissue were collected.

Figure 2. MK ameliorates the running speed, maximal hanging time and muscle mass in CKD mice at a low or medium doses.

(A) Effects of MK on HIF-1α expression in gastrocnemius muscle samples. Running speed (B) and maximal hanging time (C) in CKD mice treated with or without MK. (D) H & E staining of TA muscle. Scale Bar=50 μm. (E) Distribution of the myofiber CSA in TA muscles from CKD mice treated without or with MK. (F) Mean fiber areas of TA muscles. Data are expressed the mean ± standard error of the mean (n =6–8). *p <0.05, **p <0.01 versus Sham + vehicle group; ▲p <0.05, ▲▲p <0.01 versus CKD + vehicle. CKD, chronic kidney disease; MK, MK-8617; CSA, cross sectional area; H&E, Hematoxylin and eosin; TA, tibialis anterior.

Figure 3. MK improves mitochondrial numbers and muscle size in CKD mice.

(A) SDH staining of TA muscle. Scale Bar =50 μm. (B-C) SDH-positive fibers (dark color fibers), (B) and SDH density (C) of TA muscle in CKD mice treated with or without MK. (D) Electron microscopic observations of the quadriceps muscles. Arrows: mitochondria. Scale Bar =1 μm. (E) Quantification of mitochondrial density. (F) Quantification of mitochondrial size. Data are the mean ± standard error (n =6–8). *p <0.05, **p <0.01 versus Sham + vehicle group; ▲p <0.05, ▲▲p <0.01 versus

CKD + vehicle mice. CKD, chronic kidney disease; MK, MK-8617; SDH, succinate dehydrogenase; TA, tibialis anterior.

Figure 4. MK improves angiogenesis in the skeletal muscle of CKD mice.

(A) CD31 (red) and sarcoglycan-γ (green) staining of TA muscle in Sham-operated mice and CKD mice with or without MK. Scale Bar =40 μm. Capillary density (B) and mean capillary area (C) in TA muscle. mRNA expression of VEGF-A (D),VEGF-R1 (E) and VEGF-R2 (F) were measured by qRT-PCR. (G) VEGF-A expression assessed by western blot analysis. Data are the mean ± standard error (n =6–8). *p <0.05, **p <0.01 versus Sham + vehicle group. ▲p <0.05, ▲▲p <0.01 versus CKD + vehicle mice. CKD, chronic kidney disease; MK, MK-8617; SDH, succinate dehydrogenase; TA, tibialis anterior.

Figure 5. High doses of MK induce inflammation in the skeletal muscle of CKD mice.

(A) Macrophage infiltration in the TA muscle using F4/80 antibodies. Arrows: macrophages. Scale bar =20 μm. (B) Quantification of macrophage density in TA muscle. mRNA expression of MCP-1 (C), IL-6 (D) and TNF-α (E) measured by qRT-PCR. Data are the mean ± standard error (n =6–8). *p <0.05, **p <0.01 versus Sham + vehicle group. ▲p <0.05, ▲▲p <0.01 versus CKD + vehicle mice. CKD, chronic kidney disease; MK, MK-8617; TA, tibialis anterior.

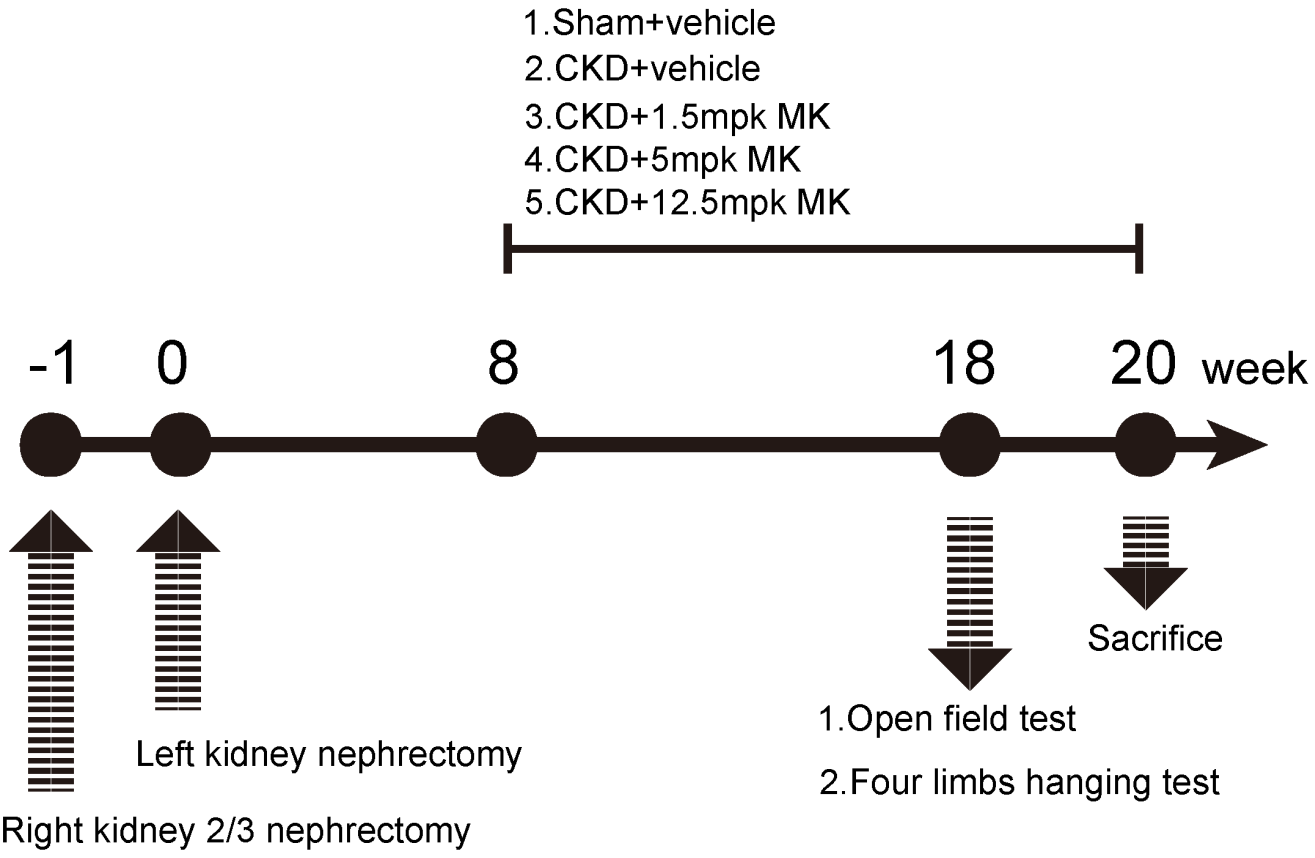

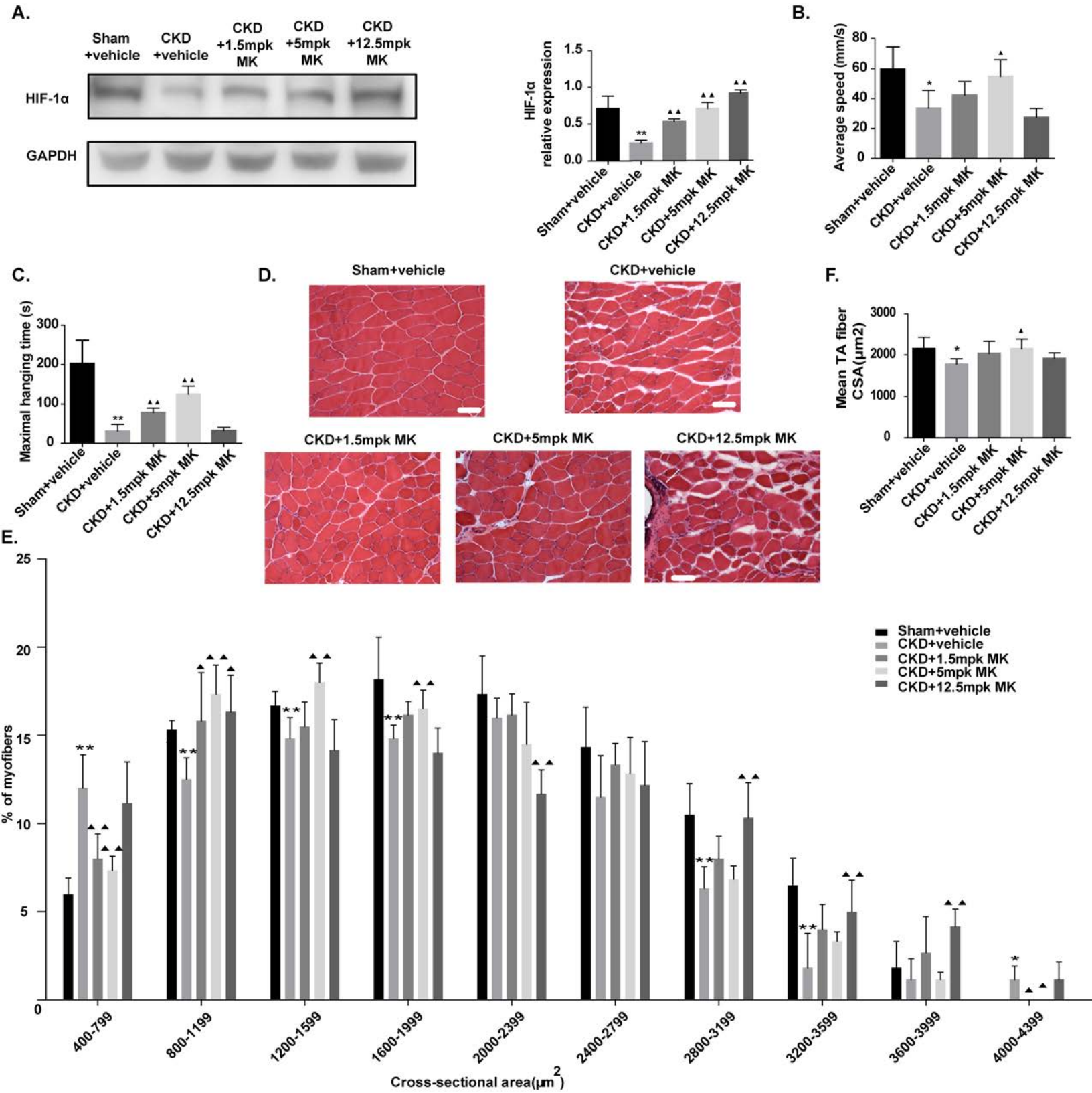

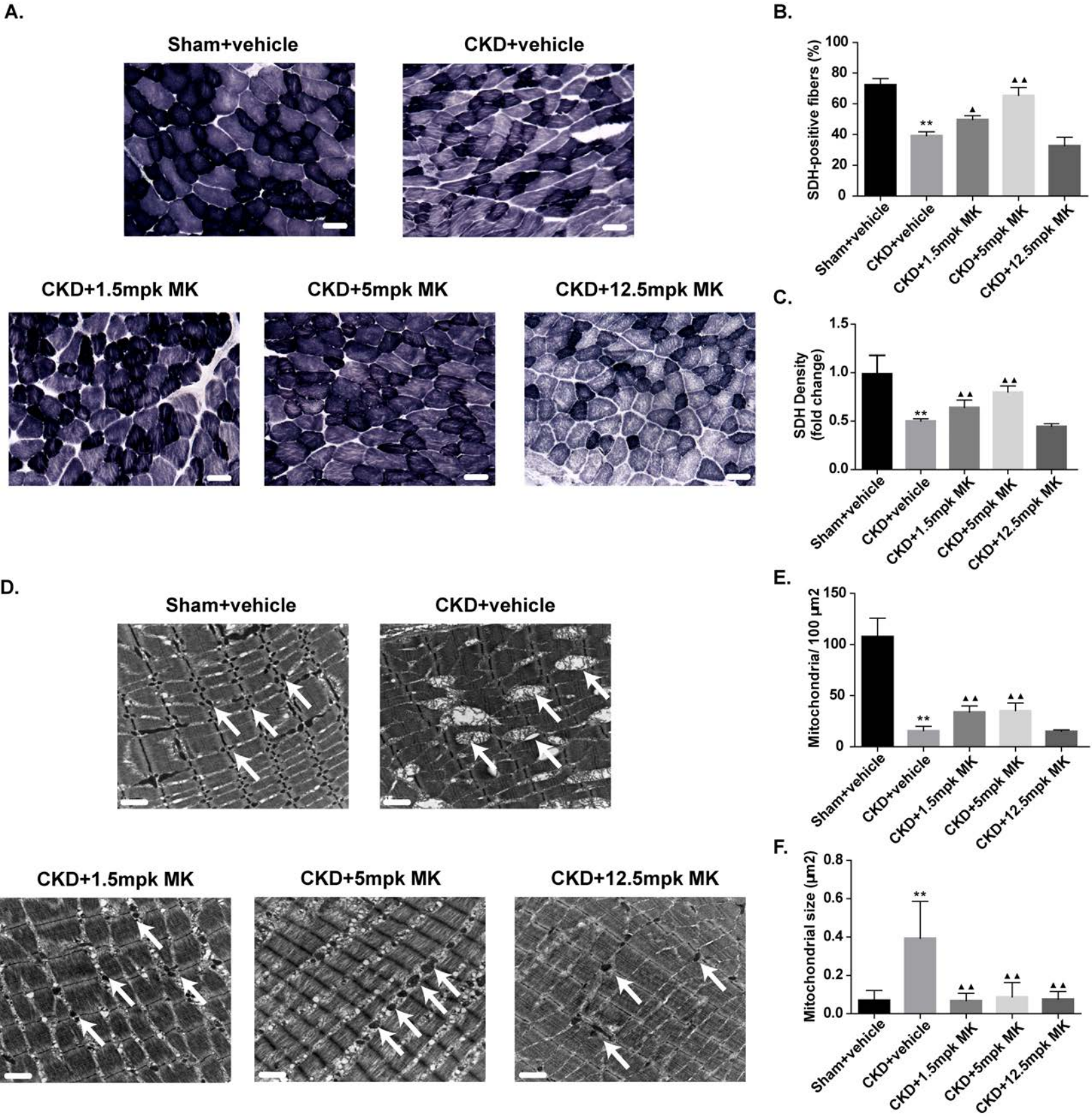

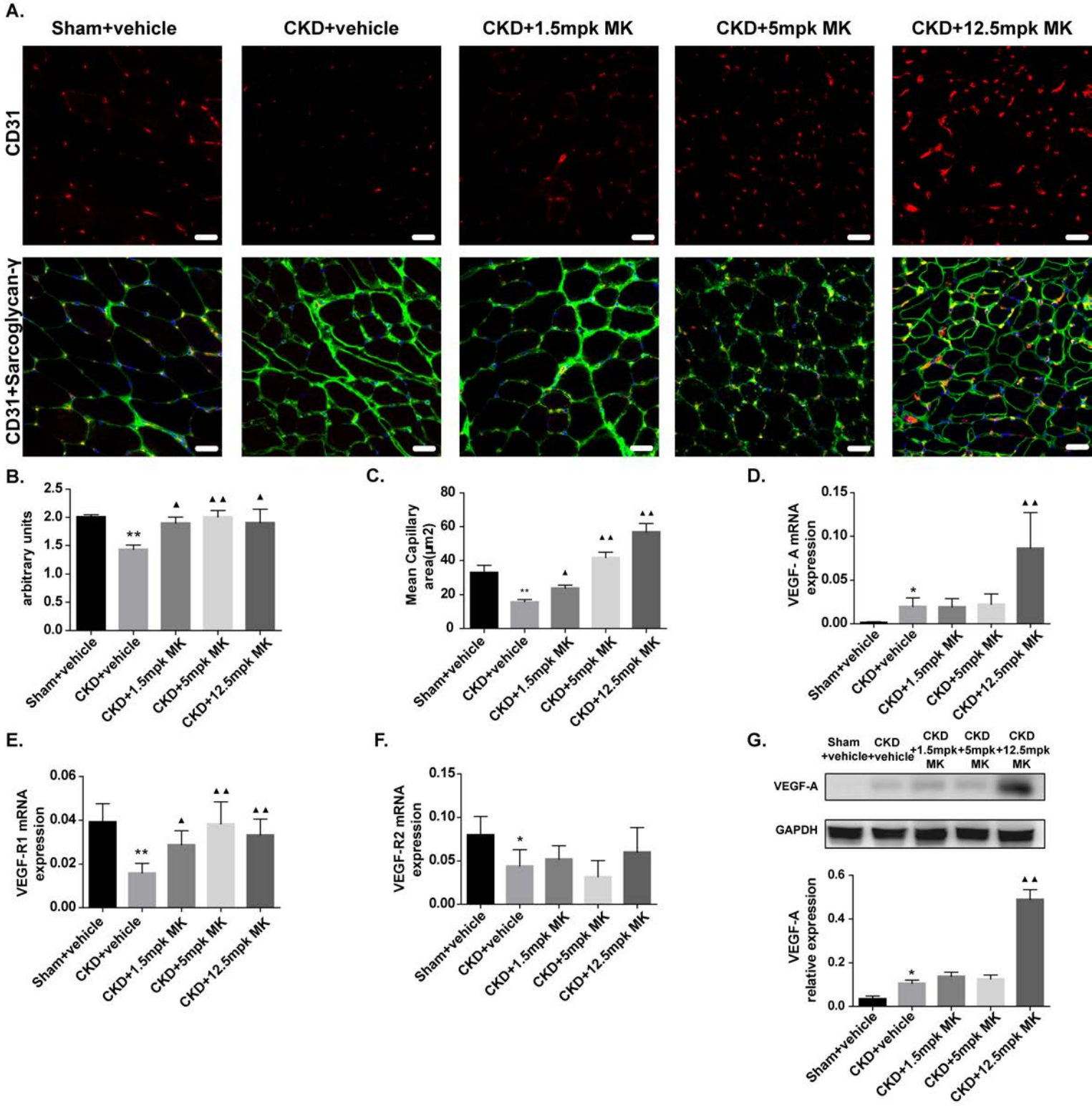

A.

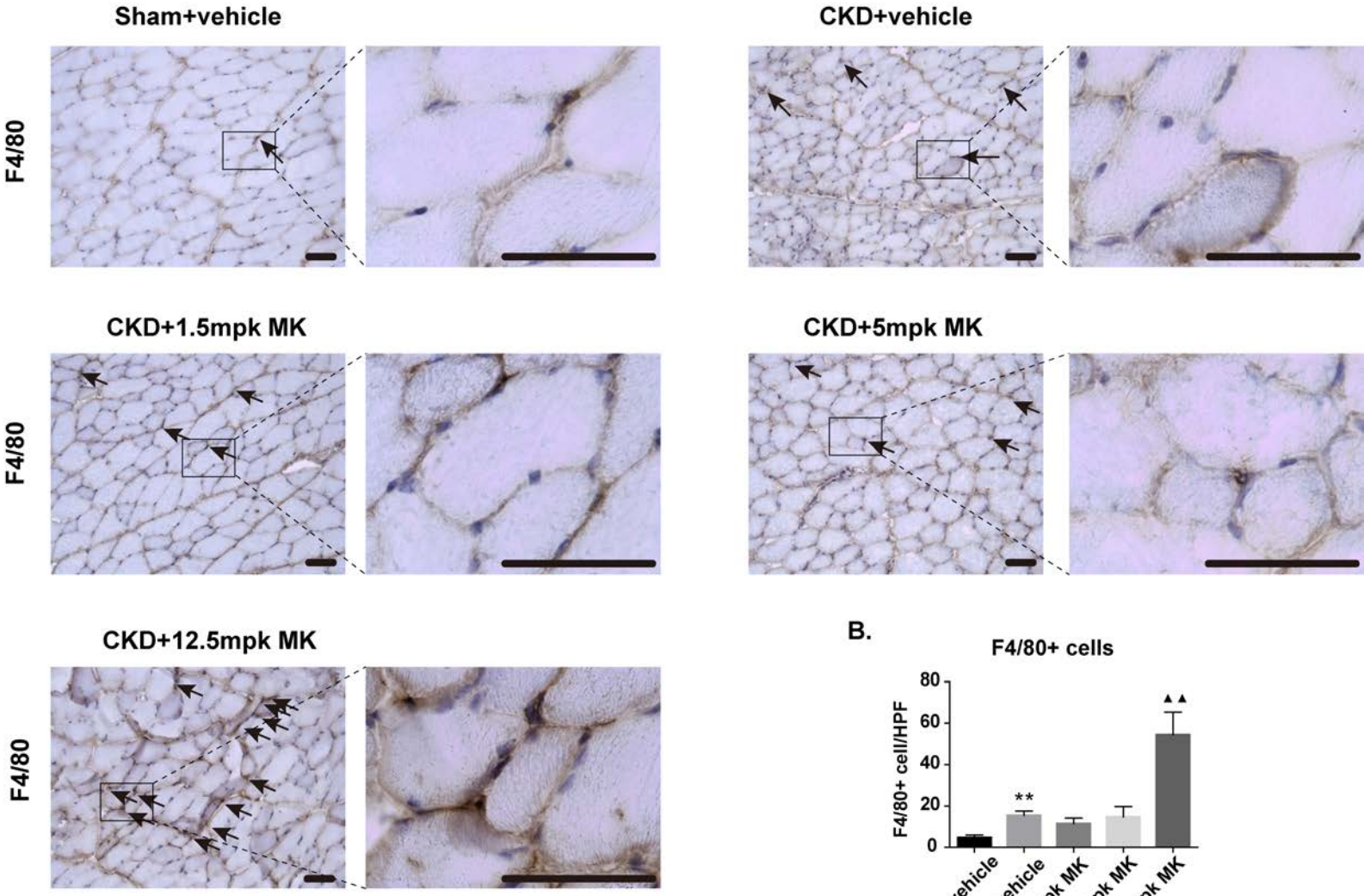

B.

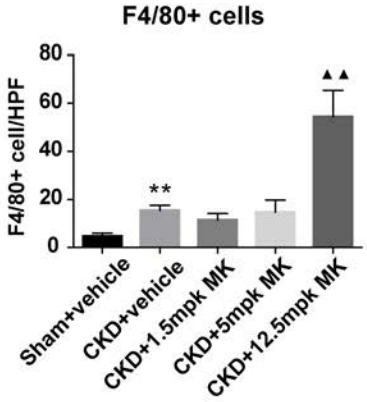

C.

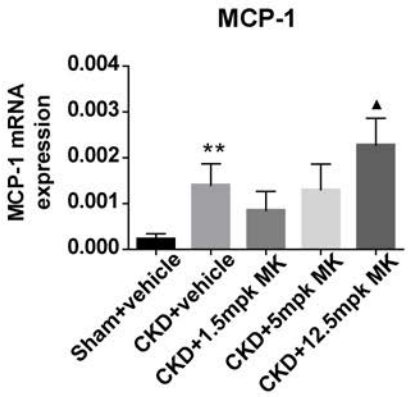

D.

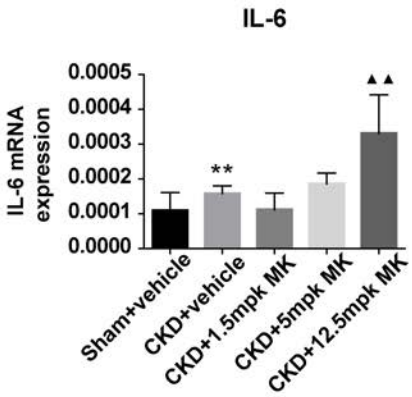

E.

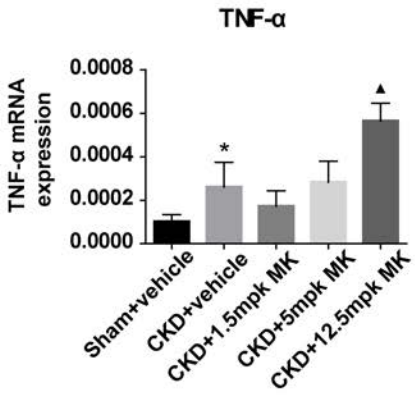

Table 1 Compare of serological parameters, body and muscles weights among Sham+vehicle, CKD+vehicle mice and MK treated mice.

	Sham + vehicle	CKD			
		vehicle	MK 1.5mpg	MK 5mpg	MK 12.5mpg
BUN(mg/dL)	11.3±0.2	25.5±3.5[b]	21.0±1.4[d]	20.2±0.8[d]	30.4±1.4[d]
SCr(mg/dL)	41.4±1.6	82.0±6.2[b]	64.6±2.0[d]	62.7±5.5[d]	91.1±5.4[c]
Final BW(g) (at 20 weeks)	30.5±2.4	23.5±1.7[b]	27.2±2.0[c]	26.9±1.1[c]	22.0±2.5
Tibialis anterior (mg)	41.4±4.0	27.8±2.4[b]	35.5±3.0[d]	37.3±3.1[d]	27.6±2.1
Gastrocnemius (mg)	122.2±7.8	78.2±6.1[b]	104.5±6.7[d]	108.9±8.3[d]	78.8±4.5
Serum EPO (pg/mL)	28.6±6.5	39.7±7.4	85.7±7.8[d]	100.4±8.2[d]	86.1±7.4[d]
Hb (g/L) (at 8 weeks)	79.1±2.2	59.9±4.6 [b]	59.5±3.4	58.1±4.7	58.4±3.1
Hb (g/L) (at 20 weeks)	77.7±2.6	53.8±2.1 [b]	71.7±2.5 [d]	71.8±3.2 [d]	66.5±1.6 [d]
Change in Hb (g/L) relative to week 8	-1.4±0.9	-4.3±2.3[a]	10.3±1.8 [d]	14.8±2.3 [d]	7.5±1.0 [d]

Data are expressed as the mean ± standard error of the mean.

[a]$p < 0.05$, [b]$p < 0.01$ compared with Sham+vehicle.

[c]$p < 0.05$, [d]$p < 0.01$ compared with CKD+vehicle..

CKD, chronic kidney disease; Sham, sham-operated mice; MK, MK-8617; BUN, blood urea nitrogen; SCr, serum creatinine; BW, body weight; EPO, Erythropoietin; Hb, hemoglobin.